Electronic Supplementary Material (ESI) for Lab on a Chip

Supplementary materials

Microfluidic chip fabrication

The fabrication of the microfluidic chip is done by using standard softlithography techniques. The master is made of SU8 photoresist (SU8-10, MicroChem) spincoated onto a silicon wafer substrate. After spinning (CEE 200, Brewer Science), prebaking, exposure to UV light (506, OAI), postbaking, and developing, the master with a thickness of 27 μm is fabricated. A mixture of the polydimethylsiloxane (PDMS) (Sylgard 184, Dow Corning) pre-polymer and curing agent (10:1) is poured over the master. After degassed, 2 hour baking, peeling off, and hole punching (0.75 μm, Harris Unicore), the PDMS layer with micro-structures is bonded to a glass substrate using a corona surface treater (BD-25, Electro-Technic Products, USA) to seal the microfluidic chip.

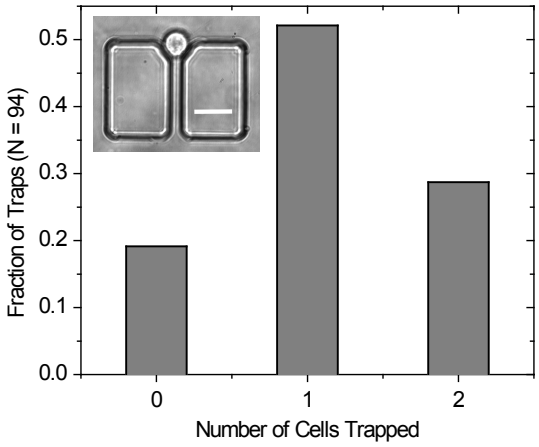

Fig. S1 Statistics of cell trapping. *N* is the number of trapping structures. The inset shows a successful trapping of a single cell. The scale bar is 20 μm.

Single cell trapping

Cells at a concentration of 10^6 cells/ml and suspended in a 0.4% trypan blue solution are pumped into the microfluidic chip at a flow rate of 0.5 μl/min. After the flow is stopped, each trapping structure may have trapped none, one, two, or even more cells. The whole process is

random. With the current design (the inset of Fig. 2), the best results have been obtained and the statistic of the number of trapped cells are provided in Fig. S1. About half of the structures trap one cell. A typical example of one trapped single myeloma cell is shown in the bright field photograph in the inset of Fig. S1.

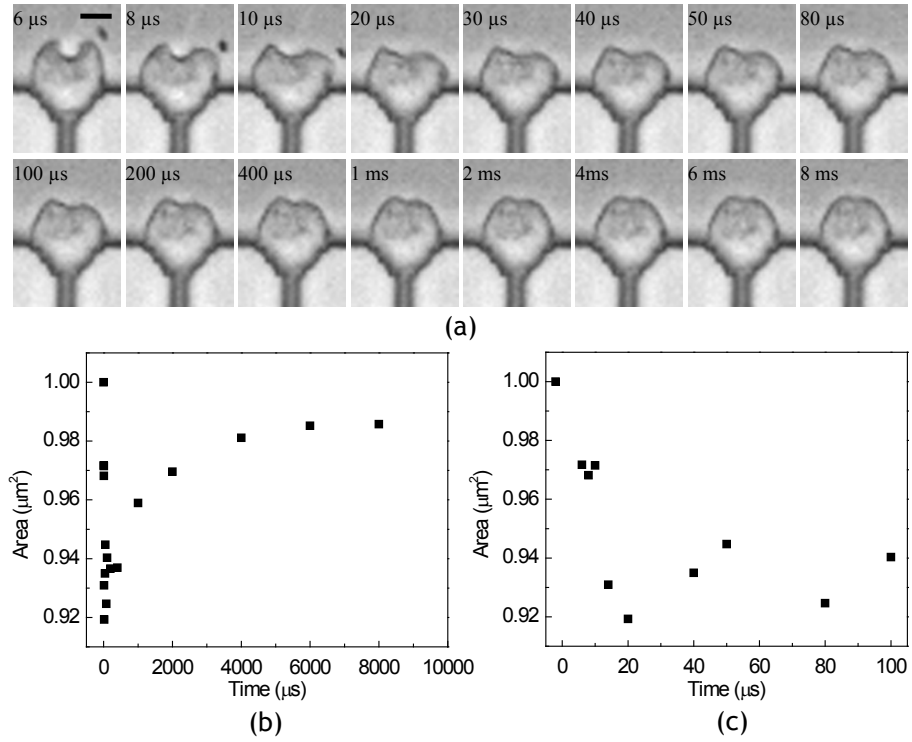

Fig. S2 The restoration process of the porated cell. (a) Selected images of the restoration process from 6 µs to 8 ms. The scale bar is 10 µm. (b) The variation of cell area vs. time and the period from 0 µs to 100 µs is replotted in (c).

Cell shape recovery

A cell recovery sequence is depicted in Fig. S2(a). The shape of the cell progressively returns to its initial shape over the course of 8 ms. The projected area of the cell is tracked and its change vs. time is plotted in Fig. S2(b). A zoom-in from 0 µs to 100 µs is given in Fig. S2(c). After the microjet poration, the area decreases to its minimum at t = 20 µs and then gradually increases back to the initial value after t = 8 ms. Considering that the volume of the cell remains constant, a reduction in the projected area means that the cell is squeezed between

the bubble and the structure, i.e. more of the cell's volume element now lies further from the symmetry axis.

Implementation of the boundary element method

The bubble is oscillating at a very rapidly, such that the flow created by it can, as a good approximation, be considered as potential flow [34-36]. There exists then a velocity potential such that the Laplace equation is valid in the fluid domain, $\nabla^2\phi = 0$, and the velocity vector is given by $\underline{u} = \nabla\phi$. Since the Laplace equation is elliptic, the solution anywhere in the fluid domain is fully determined when the potential or its normal derivative $\partial\phi/\partial n = \underline{n}\cdot\nabla\phi$ are given on the boundaries (with $\underline{n}$ being the normal vector pointing out of the fluid). Then a boundary integral formulation can be written as [37, 38]:

$$c(\underline{x}_0)\phi(\underline{x}_0) + \int_S \phi(\underline{x})\frac{\partial G(\underline{x}_0,\underline{x})}{\partial n}dS = \int_S \frac{\partial\phi(\underline{x})}{\partial n}G(\underline{x}_0,\underline{x})dS \qquad \text{A1}$$

With G the free field Green function $G(\underline{x}_0,\underline{x}) = 1/|\underline{x}-\underline{x}_0|$, $\underline{x}_0$ is a fixed point (in practice one node of the numerical mesh) and $\underline{x}$ the integration variable situated on S. S consists of two surfaces, the bubble surface and the solid surface. An axisymmetrical implementation as the one used in Ref [35] is used with a linear representation of the potential and the normal velocity on S. If $\underline{x}_0$ is situated on the surface S, c represents the solid angle at that location. If $\underline{x}_0$ is located in the fluid domain, then c=4π. After discretising the surfaces of the bubble and the solid (51 nodes each), a matrix equation relating all the potentials and its normal derivates results as ($\underline{\phi}$ and $\underline{\partial\phi/\partial n}$ represent vectors with the potential and its normal derivative for each node):

$$\underline{\underline{G}}\cdot\underline{\partial\phi/\partial n} = \underline{\underline{H}}\cdot\underline{\phi} \qquad \text{A2}$$

As shown in Ref [39], Eq. A1 can be rewritten in the following form if $\underline{x}$ is situated on the surface S:

$$\int_S [\phi(\underline{x}) - \phi(\underline{x}_0)] \frac{\partial G(\underline{x}_0, \underline{x})}{\partial n} dS = \int_S \frac{\partial \phi(\underline{x})}{\partial n} G(\underline{x}_0, \underline{x}) dS \qquad \text{A3}$$

The above formulation is equivalent to stating that each diagonal element of the matrix $\underline{\underline{H}}$, is equal to 4π minus the sum of the other elements of that row. This also eliminates the need to calculate the solid angle, c.

On the solid surface $\partial\phi / \partial n = 0$ (non penetrating condition or normal velocity is zero). On the bubble surface we will use the Bernoulli equation

$$p = p_{ref} - \rho \frac{D\phi}{Dt} + \frac{1}{2} \rho |\underline{u}|^2 \qquad \text{A4}$$

and an adiabatic function for the bubble pressure p as: $p = p_0 (V_b / V_{b0})^{\gamma}$. ρ is the density of the liquid (1000 kg/m^3), p_{ref} is the reference pressure (1 Bar), p_0 the initial pressure of the bubble (100 Bar), V_{b} the volume of the bubble, V_{b0} the initial volume, γ is the ratio of specific heats for the bubble contents (here a value of 1.25 has been chosen). Surface tension and gravity effect have been ignored. The material derivative D/Dt in Eq. A4 is used to get the potential on the bubble surface for the next time step. In Eq. A2, the potential on the bubble and the normal velocity on the solid surface are now known. The unknown normal velocity on the bubble and the potential on the solid surface can then be calculated by solving the system of equations Eq. A2. From the normal velocity on the bubble surface and the potential distribution on that surface, the velocity vector $\underline{u}$ can be calculated. With this velocity the nodes are being updated on the bubble surface (the solid surface does not move). For more details on the numerical implementation see for example in Ref [35] and [36]. The

initial radius of the bubble is chosen to be 0.14851 times the maximum bubble radius. Since the bubble is oscillating near a solid structure, a jet will be generated towards it [34].

The cell is modeled as being part of the fluid (i.e. the cell is assumed not to have much influence on the behavior of the bubble; its stresses are supposed to be negligible to the ones generated by the bubble and its density is close to the surrounding fluid). The potential in any part of the fluid (and thus also at the location of the cell) can be obtained after the potentials and normal velocities on both bubble and solid structure have been calculated with Eq. A1 by putting $\underline{x}_0$ on the location of the cell and setting c=4π. The velocity at this point can easily be obtained with $\underline{u} = \nabla\phi$ (by taking ϕ at different locations very close to $\underline{x}_0$ and calculating the gradient numerically). The cell position is updated with $\underline{x}_0^{t+\Delta t} = \underline{x}_0^t + \Delta t \underline{u}$ (Δt is the time step) and thus follows the flow field created by the interaction of the oscillating bubble and the solid structure. The cell location was monitored with 20 nodes initially evenly distributed along the cell surface.